Bonding and Interactions in UO_2^{2+} for Ground and Core Excited States: Extracting Chemistry from Molecular Orbital Calculations

Paul S. Bagus,* Connie J. Nelin, Bianca Schacherl, Tonya Vitova, and Robert Polly*

ABSTRACT: Theoretical analyses of actinyls are necessary in order to understand and correctly interpret the chemical and physical properties of these molecules. Here, wave functions of Uranyl, UO_2^{2+}, are considered for the ground state and for the core excited states where an electron is promoted from the U $3d_{5/2}$ shell into a low-lying unoccupied orbital that is U 5f antibonding with the ligand, O, orbitals. A focus is on the application of novel theoretical methods to the analysis of these wave functions so that measurements, especially with X-ray absorption, can be related to the UO_2^{2+} chemical bonding. The bond covalency is examined with these theoretical methods. The study includes how the covalent character is different for the ground and excited configurations and how this character changes as the U−O distance is changed. Furthermore, analyses are mode of how many-body effects may modify excitation energies and X-ray adsorption intensities. This includes determining the extent to which a single configuration provides a satisfactory model for the UO_2^{2+} wave functions. Two distinct types of many-body effects are considered. One involves the angular momentum coupling of the open shell electrons in the excited states to yield correct multiplets. The second adds excitations from shells that are bonding into the antibonding open shell space. These excitations are essential to properly describe the X-ray adsorption. While these many-body effects must be taken into account, their importance and their role can be explained and understood using orbitals and orbital occupations.

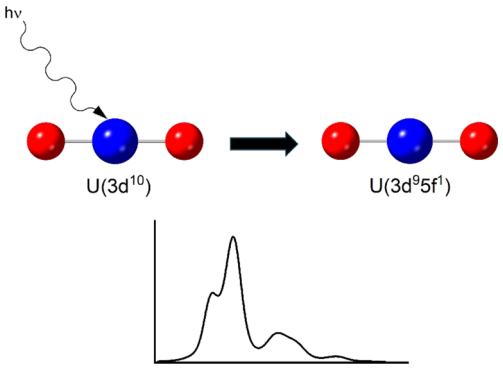

I. INTRODUCTION

The actinide elements have complex but not well understood chemical and physical properties. Yet they are important for both scientific and technological considerations.[1,2] X-ray absorption spectroscopies, both resonant inelastic X-ray scattering (RIXS) and conventional X-ray absorption spectroscopy (XAS), have been used to investigate and characterize actinides in different chemical situations.[3−5] In particular, theoretical analyses of actinyls are key to understanding and interpreting the measured XAS, especially for relating the measurements to their origin in the electronic structure. For this reason, there have been many theoretical studies of the electronic structure of actinyls and of related actinide compounds; see, for example, refs 1,2,6−15. In the present paper, we present a detailed theoretical analysis, based on wave functions, WFs, of the ground state, GS, and the excited states of uranyl, UO_2^{2+} where an electron from the U($3d_{5/2}$), M_5, shell, is promoted into the 5f shell; the excited configuration for these states is described as $M_5 \rightarrow 5f$. Our analysis significantly extends that which has been made in the previous studies cited above. In particular, we examine how the properties of the GS and the excited states change when the U−O distance is changed. Indeed, an important conclusion is that the agreement of theory and measured XAS provides a new and independent approach to determine the U−O bond distance. The theoretical XAS obtained with the wave functions, WFs, for these configurations is compared with experimental XAS data extracted from our RIXS measurements; see, for example, ref 2. We have found that the excitations from U($3d_{3/2}$) into the 5f shell, $M_4 \rightarrow 5f$, can be analyzed in a way very similar to the $M_5 \rightarrow 5f$ which we have studied and, hence, we do not include the $M_4 \rightarrow 5f$ excitations in the present paper.

An important consideration for the electronic structure is how it changes as the U−O bond distance changes and such changes are the principal focus of the present paper. This is

important since changes in the theoretical XAS predictions with bond distance, not considered in our earlier papers on the actinyls,[1,2] might be used to predict bond distances as well as providing an understanding of how the electronic structure depends on the bond distance. In particular, there is a concern about the extent to which the covalent character of the cation−anion interaction, specifically U−O, may change with the bond distance. Two important questions concern bond covalency. On one hand, one needs to explicitly define the theoretical measures that can be used to assess the extent of the covalency in UO_2^{2+} and how this covalent character changes with bond distance. There is furthermore the question of whether rigorous ab initio quantification of covalent bonding and its dependence on bond distance are needed and useful for the interpretation of the measured XAS. In the present work different theoretical models of the XAS excited states are considered and different theoretical measures of covalent character are used. In one of the theoretical models, described as Open Shell Active, or OSA, mainly the angular momentum coupling of the open M_5 and 5f shells is considered to describe the XAS excitation energies and intensities. In the second theoretical model, many electron effects are added which allow excitations from the closed valence shells of Uranyl into the open, 5f, shell space and are described as Open Closed Shell Active, OCSA.[2] While these methods have been described previously,[2] they are reviewed and applied for the analysis of the XAS for different U−O bond distances. For the analysis of the covalent character, we use the methods of orbital projection used previously[1,2] to describe the character of both orbitals and WFs. However, we also introduce new measures of how the covalent character changes with distance. These are the changes of orbital energies of levels in the 5f open shell space and the sizes of the charge distribution. It is important, as we will show later, that these different measures give consistent views of the bonding and the chemical interactions. We explicitly point out that our approach is to use these theoretical measures not so much to get the "right" answer but, rather, to obtain understanding of the character of the UO_2^{2+} excited states.

This paper is divided into the following sections: The next section, Section II, Theoretical Models and Methods, serves two purposes. The chemical and physical content of the methods that we use to characterize the extent of covalent character are reviewed and the computational programs to obtain our results are described. In Section III, Theoretical and Measured XAS, The theoretical XAS determined for different U−O distances are compared to the measured XAS[2] and the importance of the changes in the XAS with bond distance is shown. This is followed by a detailed theoretical analysis of the orbitals and WFs of both the initial GS and of the $M_5 \rightarrow 5f$ excited states with an emphasis on how they change with distance. In particular, the concern is for how these changes with distance reflect, and indicate, changes in the covalent character with distance. The paper closes with Section IV, Summary, where conclusions reached about the chemistry of the excited XAS states of UO_2^{2+} are reviewed.

II. THEORETICAL MODELS AND METHODS

The Uranyl cation, UO_2^{2+}, is a linear molecule with a U−O bond distance estimated to be between 1.76 Å[16] and 1.78 Å.[17] It is normally found in solution with various compounds[6,7,16,17] although here it will be treated as an isolated compound, an approximation that has been used successfully previously; see for example ref 6. The nominal charges of the atoms are U^{6+}, also described as U(VI), and O^{2-}; since there is considerable covalency, these nominal charges will be significantly modified. The molecule is placed along the z axis and the symmetry is $D_{\infty h}$. The $D_{\infty h}$* double group[18] is used to describe the electronic structure so that scalar and spin−orbit relativistic effects are rigorously taken into account. In order to separate chemical bonding from purely electrostatic effects models where the O anions are replaced by point charges, PCs, to form a system denoted PC-U(VI)-PC. The changes of various properties with the U-PC distance will also be considered. The U−O and U-PC distances to be studied are 1.8 Å = 3.40 bohr as a good approximation to the U−O bond distance in UO_2^{2+}[16,17] with steps of 0.1 bohr = 0.053 Å between U−O distances of 2.9 to 3.5 bohr.

The states to be considered are the closed shell ground state, GS, with a nominal U configuration of .....$3d^{10}$.....$5f^0$ where the U(3d) occupation is explicitly shown because for the excited states a 3d electron is promoted to a 5f orbital. For the excited states, the configuration is .....$3d_{3/2}{}^4 3d_{5/2}{}^5$.....$5f^1$ where the excitation is from the spin−orbit split $3d_{5/2}$ to 5f, $M_5 \rightarrow 5f$, or simply M_5. The 3d spin−orbit splitting of $3d_{3/2}$ and$3d_{5/2}$ is ∼170 eV. Thus, the excitations from the spin−orbit split $3d_{3/2}$ to 5f will be energetically well separated from and will not mix with excitations from $3d_{5/2}$ to 5f. However, the pure 5f spin−orbit splitting of an isolated U cation is ∼1 eV. This is smaller than or comparable to the splittings of the 5f orbitals in the UO^{+2} excited states where the 5fϕ and 5fδ orbitals are nonbonding, the 5fπ orbitals are antibonding and the 5fσ orbitals are strongly antibonding; see, for example ref 1. Of the excited states with these two configurations, only those that are dipole allowed from the ground state are of concern. Since the closed shell ground state in the double group has total symmetry 0_g^+, the equivalent of nonrelativistic symmetry $^1\Sigma_g^+$, the dipole allowed final state symmetries are 0_u^+ and 1_u.[18] The orbitals are 4-component spinors that are variationally optimized as the solutions of Dirac Hartree−Fock, DHF, equations.[19] The orbitals are optimized separately for the closed shell configuration of the GS and for the excited state configuration where the orbitals are optimized for the average of configuration over all possible couplings of the open shell electrons in the configuration .....$3d^9$.....$5f^1$.[20] These orbitals are then used to form many-electron configuration interaction, CI, WFs. Since the GS is closed shell, only one determinant is used and the CI WF for the GS is simply the DHF WF. Since the excited states have open shells, the choice of the determinants to be included in the CI WFs is more complicated.

The determinants in the excited state CI WFs assume a core of orbitals that are occupied in all the determinants in the CI. The orbitals which may have different occupations in the various determinants are described as spaces formed with two parameters: the first parameter describes the orbitals that will be used to form the determinants and the second parameter describes how these orbitals will be occupied in the determinants. For the excited states of UO_2^{2+}, a simple set of spin−orbitals are the 6 $3d_{5/2}$ and the 14 5f from which the occupied orbitals are selected with the constraint that 5 of the 6 $3d_{5/2}$ and 1 of the 14 5f are occupied. It is straightforward to determine that for $M_5 \rightarrow 5f$ excitation this leads to 12 nondegenerate excited multiplets with 0_u symmetry and 11 doubly degenerate excited multiplets with 1_u symmetry. The 12 0_u multiplets are divided into 6 0_u^+ multiplets where

excitations are allowed and 6 0_u^- which are symmetry forbidden, This is denoted as an Open Shell Active, or OSA, space.[2] The excited OSA WFs are investigated to determine if they can be viewed following the picture of "one-electron" excitations into the 5fϕ, 5fδ, 5fπ, and 5fσ as has been proposed earlier.[21] The second CI space involves an additional set of orbitals chosen from the bonding closed shell orbitals which have significant 5f character. This has been described as an Open Closed Shell Active, or OCSA, space which is divided into three subspaces. As in the OSA case, there are 6 $3d_{5/2}$ spin−orbitals in the first subspace and 14 5f spin orbitals in the second sub space, but now there are 6 spin−orbitals from the closed shells in the third subspace. These 6 spin−orbitals from the closed shell space are chosen on the basis of the extent of 5f bonding character in these orbitals.[1,2] They have been chosen because 95% of the U(5f) character in the UO_2^{2+} closed shell orbitals is contained in them. Within these three OCSA orbital subspaces, excited configurations with the following three sets of distributions of electrons are allowed: (1) There are 5 in the first, $3d_{5/2}$, subspace, 1 in the second, 5f, subspace, and 6 in the third, closed shell, subspace; this is identical to the OSA configuration space. (2) Single excitations from the new, third subspace into the second, 5f subspace are allowed with 2 electrons in the 5f subspace and 5 electrons in the third "closed" shell subspace. (3) In addition, double excitations are also allowed from the third subspace so that there are 4 electrons in this space and 3 electrons in the 5f subspace. For $M_5 \rightarrow$ 5f excited states, the number of OCSA multiplets with 0_u symmetry increases to 3616 where the dipole allowed 0_u^+ symmetry should be 1808 and the number of OCSA multiplets with 1_u symmetry increases to 3511.

For these WFs, we briefly review their dipole XAS intensities for the $M_5 \rightarrow$ 5f X-ray Absorption Spectra, XAS, as described in ref 2 where the XAS was examined only for the nominal U−O distance of 1.8 Å. We take the relative dipole transition intensities, I_{rel}, from the nondegenerate closed shell initial state, described by $\Psi(GS)$, to a particular final state, Ψ_f denoted with the index f, as, simply

$$I_{rel}(f) = |\langle \Psi(GS)|\mathbf{r}|\Psi_f\rangle|^2 \quad (1)$$

Where we neglect the term in the cube of the transition energy between $\Psi(GS)$ and Ψ_f[22] since the excitation energy from GS to the excited states is ∼3600 eV[23] and the energy range over the different final states is less than 20 eV.[21] Hence, the neglected factor in the transition energy is almost constant over the energy range of interest. In the present work, we examine the XAS for different U−O distances and show that there is a strong dependence of the XAS, with both the OSA and OCSA WFs, on the U−O distance. The dipole intensity matrix elements of eq 1 are computed rigorously, taking into account the different orbitals determined for the initial, GS, and $M_5 \rightarrow$ 5f configurations[24] as well as the different CI WFs for the various excited states. For the XAS plots, we broaden the calculated dipole intensities with a Voigt convolution[25] of a Gaussian with Full Width at Half Maximum, FWHM, of 1.0 eV and a Lorentzian with FWHM of 3.5 eV for the M_5 lifetime. The Gaussian FWHM was chosen as a very rough measure of the experimental resolution for the specific geometry of the measurements and the Lorentzian FWHM for lifetime of an M_5 hole in U was taken from the compendium of Campbell and Papp.[26] This choice of broadening should only be regarded as a rough approximation that allows us to directly compare our theoretical predictions for the XAS with the measured XAS obtained from suitable slices of the Resonant Inelastic X-ray Scattering, RIXS, maps.[2] We show that our theoretical predictions for the XAS for different U−O distances provide a basis for understanding how the electronic structure, in particular the covalent character of the U−O interaction, may modify the XAS at different U−O distances.

Several properties of the orbitals and WF are examined. One set of properties comes from the projection of orbitals of the isolated U(VI) cation on the orbitals of UO_2^{2+}. For UO_2^{2+}, the interesting U orbitals are the 5f and 6d frontier orbitals. We recall that the projection of the 5f character of an orbital, $N_P(i,5f_\lambda)$ is

$$N_P(i,\ 5f_\lambda) = |\langle U(5f_\lambda)|\varphi_i\rangle|^2 \quad (2)$$

where φ_i is the i^{th} DHF orbital obtained for either the GS or the $M_5 \rightarrow$ 5f excited configuration of UO_2^{2+}, U(5fλ) is a $5f_\lambda$ orbital of an isolated U cation and $\langle U(5f\lambda)|\varphi_i\rangle$ is the overlap integral, including spatial and spin coordinates, between these orbitals. The possible range of $N_P(i,5f_\lambda)$ is

$$0 \le N_p(i,\ 5f_\lambda) \le 1 \quad (3)$$

where $N_P(i,5f_\lambda) = 0$ indicates that the orbital φ_i has no $5f_\lambda$ character and $N_P(i,5f_\lambda) = 1$ indicates that the orbital is a pure $5f_\lambda$ orbital. Both the $5f_\lambda$ and the i orbitals are doubly degenerate and the projections are taken for the combination with nonzero overlap. The projection is taken both for the orbitals of the valence open shell, in the excited configuration and also for the closed shell orbitals of both the GS and the excited configuration. Projections on the closed shell orbitals are taken to obtain information about the occupations of the 5f in the bonding closed shell orbitals. Equivalent projections on the closed shell UO_2^{2+} orbitals are also made for the U(6d) orbitals. These projections provide information about the covalent character of the closed shell, bonding orbitals as well as the open shell 5f antibonding orbitals. The UO_2^{2+} orbitals have gerade, g, and ungerade, u, symmetry in the $D_{\infty h}$* symmetry of the linear molecule; thus, the projections of U(6d) will give information about the covalent character of the g orbitals while the U(5f) projections give information about the u orbitals. Since U is nominally U^{6+}, the orbitals of the U cation used for the projection are the unoccupied 5f and 6d of this cation. However, we have also tested using the 5f and 6d orbitals occupied in the U^{2+} cation with open shell configuration 5f(3)6d(1), which are slightly more diffuse than the virtual orbitals of U^{6+}. While the absolute values of the projections are slightly larger with these orbitals, the trends of the projections for different states and for different U−O distances are virtually identical whether we use cation orbitals from U^{6+} or U^{2+}.

We also examine the composition of the OSA and OCSA CI WFs for the excited $M_5 \rightarrow$ 5f configuration to determine the orbital occupations, w(orbital), in the different WFs. For the OSA excited state WFs, all configurations have 5f occupation which is 1 but some configurations may have occupations of different $5f_\lambda$ orbitals where λ takes the values σ (or $\sigma_{1/2}$), π (or $\pi_{1/2}$ or $\pi_{3/2}$), δ ($\delta_{3/2}$ or $\delta_{5/2}$), or ϕ ($\phi_{5/2}$ or $\phi_{7/2}$). The weight of an individual $5f_\lambda$ orbital, w(5fλ), in a particular OSA WF is the sum of the square of the CI coefficients of the configurations where that $5f_\lambda$ orbital is occupied. Clearly, since one of the $5f_\lambda$ orbitals is occupied in all configurations, the sum of the w(5fλ) over all λ must be 1. If one w(5fλ) = 1 and the other 3 weights

are 0, the WF is a pure M_5 excitation to that $5f_\lambda$ orbital; if the weights are fractional, then the WF is a combination, given by the values of w(5fλ), of excitations into the different $5f_\lambda$ orbitals. In particular, the WFs with fractional w(5fλ) cannot be described by a single determinant or configuration but are CI WFs with excitations of 3d electrons into different $5f_\lambda$ orbitals. While we could consider separately the 7 individual split-orbit split 5f orbitals, it is simpler to group them together. For an OCSA excited state WF, a configuration may have an occupation of 5f orbitals that is 1 if the three closed shell orbitals have an occupation of 6 electrons; i.e., no excitation from closed shells to the valence open shell space. It may also have an occupation of 2 5f orbitals with 1 electron excited from the closed shells which now have an occupation of 5 electrons or 3 5f orbitals with the closed shells having an occupation of 4 electrons. For these WFs, the sum of the w(5fλ) may be greater than one but the weight of the occupation of the closed shells, w(closed) must also be considered and the sum of w(closed) plus the w(5fλ) will equal 7. It is useful to use Δw(closed) = w(closed)-6 so that the sum of w(5fλ) and Δw(closed) is again equal to one. It is worth recalling that these weights are not for pure U cation 5f orbitals but for the covalent antibonding orbitals that are used for the OSA and OCSA CI WFs.

Another property of orbitals that are considered are the orbital energies, ε, of the open shell, dominantly 5f, orbitals, especially as a function of U−O distance. The logic here is that when the antibonding covalent character of an open shell orbital is greater, the higher, less negative, the ε will be. One can examine the different $5f_\lambda$ orbitals for a given bond distance to determine the extent of their covalent character and one can also examine the variation of the orbital energies as a function of the U−O separation. However, as one varies the bond distance, it is necessary to separate changes in the ε due to the electrostatic potential of the O anions from the changes in ε due to changes in the covalent character of the orbital due to different bonding as the U−O distance changes. For this purpose, we will compare changes in the ε's for a U cation moving in the potential due to point charges with the changes in the ε's for UO_2^{2+}. A second orbital property to be considered is the expectation value of z^2, $\langle z^2 \rangle$ where z is taken with respect to the U center as the origin. Thus, large values of $\langle z^2 \rangle$ indicate significant amount of charge centered on the O anions while small values of $\langle z^2 \rangle$ indicate reduced or little O character. In earlier work,[1,2] the $\langle z^2 \rangle$ was examined only for the valence open shell, dominantly 5f, orbitals. In the present work, we also examine the $\langle z^2 \rangle$ for the closed shell orbitals; rather than examine individual closed shell orbitals, we sum the values over the total occupation of the closed shell orbitals in the OSA WF separating only the sums for the even, g, orbitals and for the odd, u, orbitals. This separation allows us to distinguish the contributions of the U(6d), in the g orbitals, from the contributions of the U(5f) in the u orbitals. These $\langle z^2 \rangle$ are also compared between the closed shells of the initial GS and the $M_5 \rightarrow$ 5f configurations of the excited states. Thus, as well as the projections of the U(5f) and U(6d), the $\langle z^2 \rangle$ are used to examine whether and to what extent the bonding covalent character changes between initial and the excited configurations. It is necessary that these two measures provide consistent descriptions of the covalent character of the orbitals. In particular, an important use of the closed shell values of $\langle z^2 \rangle$ will be for how the closed shell covalency changes as a function of the U−O distance. We define the "closed" shells as those used for the OSA CI wave functions since then we do not have to include changes in occupation due to the excitations from a fraction of the orbitals in these shells as in the OCSA CI WFs. This is to allow us to have a direct comparison for the changes of these orbitals between the GS and the excited configurations.

While it is not a computational challenge to determine the CI WFs and the dipole XAS intensities[2] for these numbers of multiplets, it is a challenge to describe the properties of such a large number of states, especially for the OCSA WFs. Thus, we divide the multiplets of the excited states into groups with energies belonging to the group. The groups are 0.5 eV increments, ΔE, with the group energy. $E_n(G)$ given as

$$E_n(G) = E_0 + (n-1) \times (\Delta E) \tag{4}$$

where E_0 is the lowest energy for the CI calculation, either OSA or OCSA. The properties of the wave functions are summed or averaged for states with the CI energies, E(CI), in the ranges

$$E_n(G) \leq E(\mathrm{CI}) < E_{n+1}(G) \tag{5}$$

In general, our concern will be for relative group energies, $\Delta E_n(G)$, where ΔE_0 is taken as zero for the lowest energy of the excited OSA or OCSA CI WFs. The intensity in these groups is summed over the XAS dipole intensities for all the CI states in the group. The occupations of the orbitals in a group are the weighted average of the occupations, w(5fλ) and Δw(closed), defined above. The weighting in the average for a particular multiplet in the group is the intensity for that multiplet normalized by the total intensity within the group. Clearly, each of the OSA excited configurations has exactly these values of w($5f_\mu$) = 1 and w($5f_\lambda$) = 0 and it is possible to describe them as $M_5 \rightarrow 5f_\mu$. Of course, when different excited configurations are mixed in the wave functions of the excited multiplets, the integral values are lost. Furthermore, the OSA wave functions in a given group may have different dominant excited configurations from each other. However, for the special case of a group where one of the average w($5f_\mu$) is nearly 1 and the other average w(5fλ) are nearly 0, it is possible to assign this group as $M_5 \rightarrow 5f_\mu$. Unfortunately, as will be shown shortly, it is not often that such an assignment is possible. For the OCSA groups, an additional requirement is that the w(closed) in that group be nearly zero indicating that the contribution of excitations from the closed shells into the valence open shell space are small in order for the excitation to be described as $M_5 \rightarrow 5f_\lambda$.

III. THEORETICAL AND MEASURED XAS

We discuss the $M_5 \rightarrow$ 5f XAS with a primary interest in demonstrating the changes in the predicted spectra for three different U−O distances; similar dependence on the U−O distance has also been found for the $M_4 \rightarrow$ 5f XAS. The properties of the $M_5 \rightarrow$ 5f XAS have been discussed in our earlier paper for the nominal U−O distance of 1.77 Å.[2] Here we report the XAS for three different U−O distances. In Figure 1. we compare the XAS for $M_5 \rightarrow$ 5f for d(U−O) = 1.6, 1.7, and 1.8 Å obtained with OSA WFs for the excited states. In Figure 2, we give equivalent XAS plots obtained with OCSA WFs; in addition, in Figure 2, we include the high resolution XANES derived from our RIXS data, see ref 2 for details of these measurements. For the choice of the broadening parameters used to obtain the theoretical plots in these

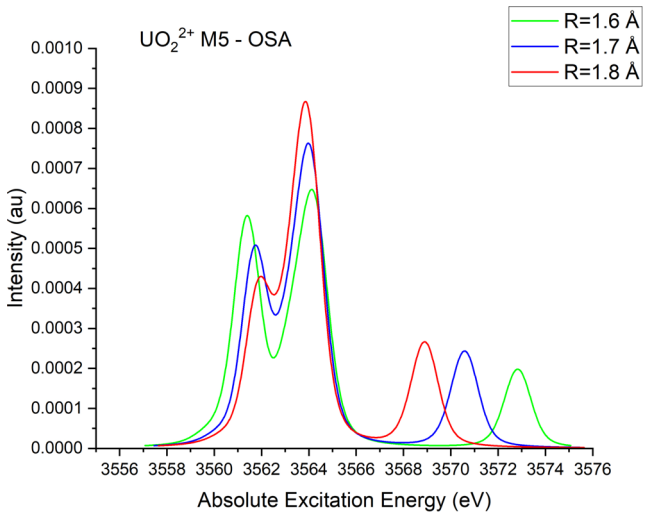

Figure 1. Plots of the $M_5 \rightarrow 5f$ XAS obtained with the OSA excited state WFs for d(U−O) = 1.6, 1.7, and 1.8 Å.

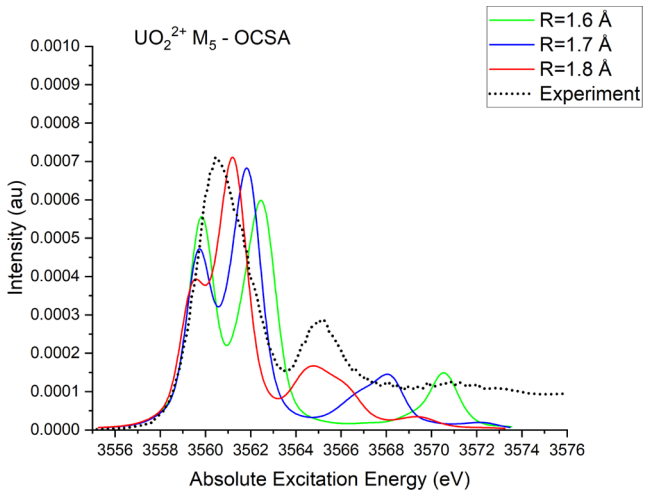

Figure 2. Plots of the $M_5 \rightarrow 5f$ XAS obtained with the OCSA excited state WFs for d(U−O) = 1.6, 1.7, and 1.8 Å including the measured XAS.

figures, see the discussion in Section II. For all distances, the OSA plots in Figure 1 have three features which, following the logic in ref 21, would be assigned as follows: The first, lowest excitation energy, peak contains unresolved excitations of an electron from $3d_{5/2}$ to $5f\phi$ and $5f\delta$. The second feature contains excitations to $5f\pi$ where the splitting of the $5f\pi_{1/2}$ and $5f\pi_{3/2}$ is not resolved; this is somewhat surprising since the spin−orbit splitting of the $5f\pi$ orbital energies is almost 1 eV.[1] The third feature is assigned as excitation into the $5f\sigma_{1/2}$ orbital. The theoretical OSCA XAS plots in Figure 2 also have three features where it is tempting to make the same assignments for the excited states as for the OSA spectra in Figure 1. The measured high resolution XAS, the dotted curve in Figure 2 has only two features but the first feature is very broad with a FWHM of ∼2 eV and it might contain unresolved contributions from excitations of $3d_{5/2}$ into $5f\phi$, $5f\delta$, and $5f\pi$ orbitals. For the measured XAS in Figure 2, there is also a broad but low intensity peak at ∼12 eV higher in excitation energy than the maximum of the first feature. The feature can be observed in Figure 2 for the plots for d(U−O) = 1.7 and 1.8 Å; for d(U−O) = 1.6 Å, the intensity is low and at higher excitation than used in the plot. This weak high excitation energy feature is also present in the measured XAS. The origin of this peak cannot be explained on the basis of a simple excitation of a 3d electron into a $5f\lambda$ orbital and suggests that these assignments may not be correct, especially for the OCSA excited state WFs. These assignments will be examined in detail below in terms of the character of the WFs and it will be shown that they are incomplete.

The character of the excited WFs is described for groups of excited states over an energy range of 0.5 eV as explained in Section II. The properties examined are the summed XAS intensity over all the states in the group and intensity weighted occupations of the 5f orbitals in the states within the group. In the figures that follow, the group intensities are shown as a yellow vertical bar. The occupations of the nonbonding $5f\phi$ and $5f\delta$ orbitals summed over their spin−orbit splittings are summed and shown as a blue circle, the occupations of the $5f\pi$ orbitals summed over $5f\pi_{1/2}$ and $5f\pi_{3/2}$ are shown as a red triangle and the occupation of the $5f\sigma$ as a green diamond. For the OCSA WFs, the occupation of electrons promoted from the closed shell space to the $5f\lambda$, Δw in Section II, is shown as a black circle. The properties for the nominal d(U−O) = 1.8 Å,[2] shown for OSA excited WFs in Figure 3 and for OCSA excited WFs in Figure 4, are reviewed. Then changes in the properties when the distance is different are considered where the properties of the OCSA excited states for d(U−O) = 1.6 Å are shown in Figure 5. In these figures, regions with different properties are enclosed in boxes.

For the OSA WFs in Figure 3, the intensities are in three regions. The first region has two features, a very low intensity feature at group energy $E(G)$ = 0.5 eV and a much more intense feature at $E(G)$ = 2.5 eV where both features have very large occ($5f\phi\delta$) ≈ 1.0. However, the more intense feature has small occ($5f\pi$) and tiny occ($5f\sigma$). Clearly the intensity in this region can be described as intensity from excitation $M_5 \rightarrow 5f\phi\delta$. The features in the second region have a large, nearly 1.0, occupation for $5f\pi$ although there is a small contribution from $5f\phi\delta$ occupations. Also, there are three groups with significant intensity rather than two as would be expected for excitations of an electron from 3d into either $5f\pi_{1/2}$ and $5f\pi_{3/2}$ which are split by ∼1 eV.[1] Furthermore, since both of the $5f\pi$ orbitals are doubly degenerate, one would expect the two peaks to have comparable intensity rather than one being twice as intense as the other two. This is a clear demonstration that, even with this simple model, one cannot describe the excitations as simply the excitation of an electron from a core orbital into a $5f\pi$ orbital but that one needs to take into account the angular momentum coupling of the electrons in the two open shells.[2] The different energies and intensities are masked in the XAS plotted in Figure 1 by the large Voigt broadenings that prevent different excitations from being resolved; clearly, this is a limitation of XAS spectroscopies. Unlike the region with π excitations, excitations from 3d into the $5f\sigma$ orbital is dominated by a single feature at a relative group energy of ∼10 eV. Overall, for the OSA excited states, it is possible to describe XAS regions as dominated by excitations into particular symmetry $5f\lambda$ orbitals, as marked in Figure 3, although there are limitations, even here, to a simple model of a one electron excitation. Clearly, the simple OSA model, shown in Figure 1, does not accurately describe the measured XAS.

In Figure 4, the group properties of the excited states with the more accurate OCSA model for the excitations are shown.

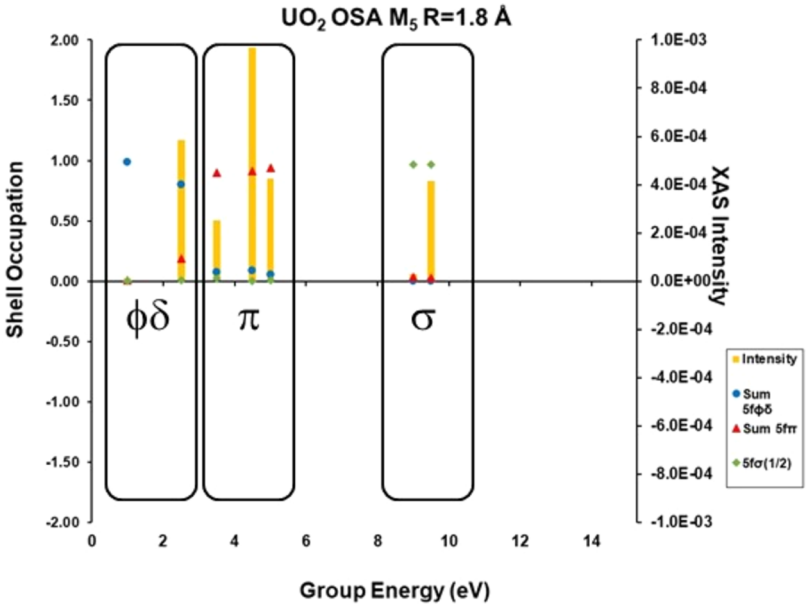

Figure 3. Plots of the properties of the $M_5 \rightarrow 5f$ excited state OSA WFs for d(U−O) = 1.8 Å; symbols for the properties are given in a box in the figures and described in the text.

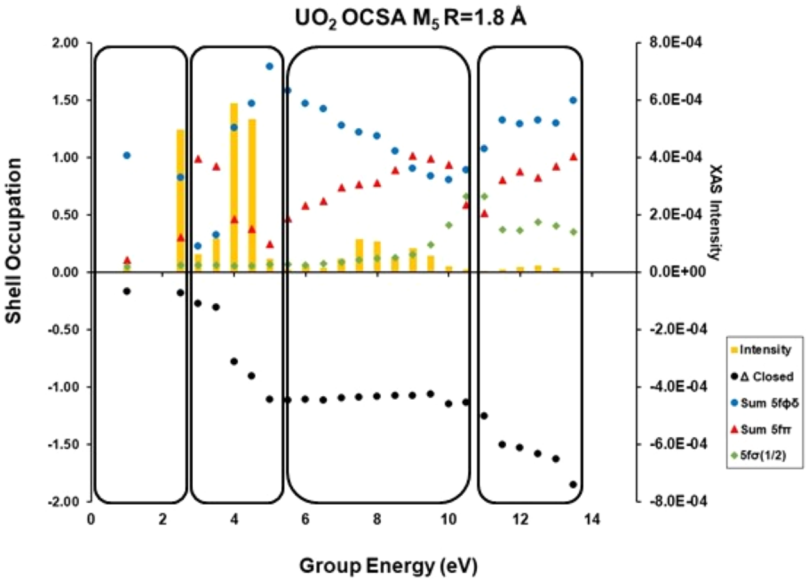

Figure 4. Plots of the properties of the $M_5 \rightarrow 5f$ excited state OCSA WFs for d(U−O) = 1.8 Å; symbols for the properties are given in a box in the figures and described in the text.

It is possible to divide the groups into regions, four instead of the three used in Figure 3, where the regions are ordered in excitation energy with the first region having the lowest excitation energy. For this first region, the excitations are still mainly in a single group dominated by occupation of $5f\phi\delta$ although there is small excitation, ~0.1 electron, from the closed valence shells into the 5f open shells. There is also a modest occupation of the $5f\pi$ orbitals. The OCSA properties in the second region are more different from the OSA properties in this region. While the two groups in this region with large intensity have large $5f\pi$ occupations, there is even larger occupation of the $5f\phi\delta$ orbitals and there is a large promotion of electrons from the closed shells into the 5f space. The occupations of the $5f\pi$ and $5f\phi\delta$ and the δw(closed) are sufficiently large that one cannot describe the excited states in this region as being represented by an $M_5 \rightarrow 5f\pi$ excitation. The many-electron, many-configuration character of the states in the third and fourth regions involves groups with large occupations in all the $5f\lambda$ orbital and large magnitude $\Delta w(\text{closed}) \lesssim -1.0$. In the third region, the intensity is distributed over a large number of groups consistent with a broad feature in the $M_5 \rightarrow 5f$ XAS, see Figure 2. The fourth region has low intensity but is observed in the measurements, Figure 2. Overall, the OCSA theoretical analysis leads to a spectrum fully consistent with the measured XAS and it shows clearly that the description of the excited states as $M_5 \rightarrow 5f\pi$ or $M_5 \rightarrow 5f\sigma$ is a serious oversimplification that neglects their true many-electron, many configuration character of the excited states.

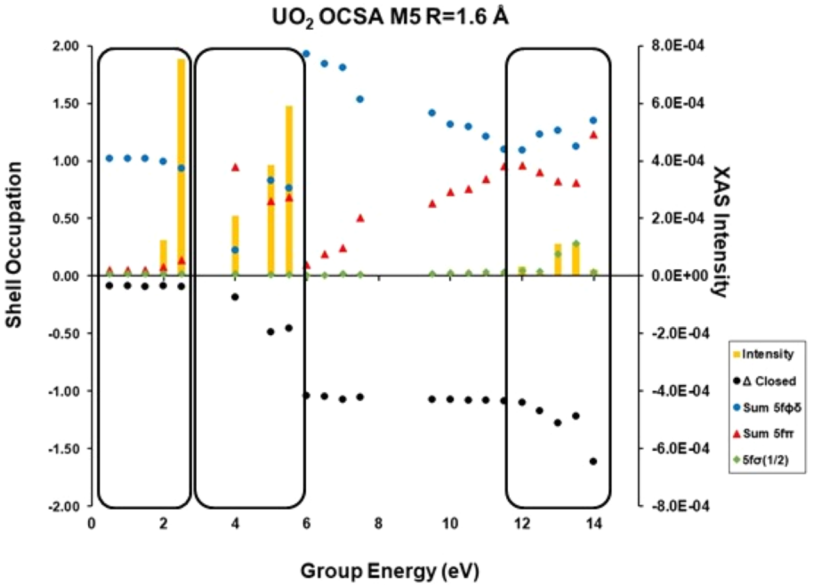

Figure 5. Plots of the properties of the $M_5 \rightarrow 5f$ excited state OCSA WFs for d(U−O) = 1.6 Å; symbols for the properties are given in a box in the figures and described in the text.

In Figure 5, the character of the excited states is examined for a shorter distance of d(U−O) = 1.6 Å where we would expect the covalent character of the orbitals to be larger. The differences of the properties are exceptionally large. For the relative group energy range shown in Figure 5, only three regions are shown where the third region has been moved to $\Delta E(G)$ in the range of 12 to 14 eV. This is done since there is very little intensity for the groups with $\Delta E(G)$ between 8 and 12 eV. The two intense groups in this third region do have the largest w(5fσ) occupation but they also have even larger occupations w(5fλ) and large magnitudes of Δw(closed). There is also a fourth region with low intensity but now for $\Delta E(G)$ between 18 to 25 eV and not shown, in part because the intensity is distributed over a large number of groups. It is appropriate to use other measures to assess the covalent character of the orbitals and how this character changes with distance.

The orbital energies of the open shell 5f orbitals provide an indication of the covalent character of these orbitals, especially of how the covalent character may change with the U−O bond distance. We expect that as the bond distance decreases the covalent character will increase and as d(U−O) increases the covalent character will decrease. As the antibonding character of the open shell, dominantly U(5f), orbitals increases, the DHF orbital energy will become larger, less negative, with the reverse change for a decrease of antibonding character; see the discussion in Section II. In addition to the change in orbital energies due to changes in bonding character with distance, these orbital energies will also change due to the electric field of the O anions at the position of the U cation. The electrostatics of the O anions' electric field acts to raise the open shell orbital energies since they have dominantly U(5f) character and clearly this electric field depends on d(U−O). As a first approximation, we can take the electrostatic change in the $\varepsilon(5f\lambda)$ as the field at the U nucleus due to the O anions. In atomic units, this potential can be taken as $2Q/d$ where Q is the effective charge of the O anions and the factor of 2 is because there are 2 anions. In order to separate the electrostatics from the covalent bonding, the $\varepsilon(5f\lambda)$ for a model of the U(VI) cation in the presence of point charges, PCs, replacing the O anions, $U(PC)_2$, is used. The charge of the PC's is taken as −1.5 rather than −2, the nominal charge, to represent the presence of covalent bonding between the U cation and the O anions. For this model changes in the $\varepsilon(5f\lambda)$, shown in Figure 6, can be due only to the electric field of the

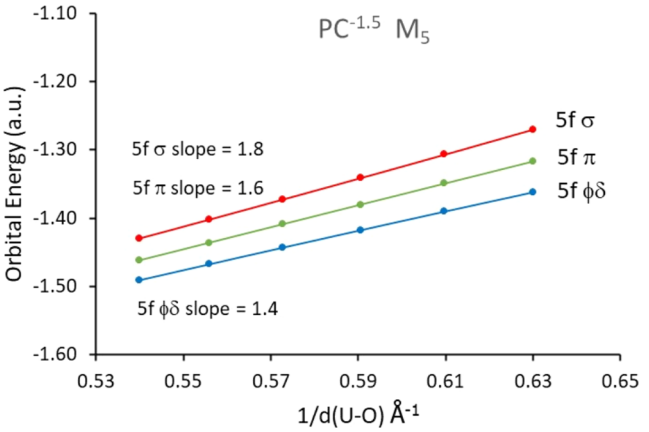

Figure 6. Plots of the 5fλ orbital energies, $\varepsilon(5f\lambda)$ in hartrees, for an excited $M_5 \rightarrow 5f$ U(IV) in the presence of point charges of Q = −1.5, denoted $U(PC)_2$, for different d(U-PC). The plots are for values of 1/d(U-PC) in $Å^{-1}$ corresponding to d(U-PC) between 1.6 to1.85 Å. see text.

PCs since no chemical bonding is possible. In order to simplify the plot, average values of the $\varepsilon(5f\lambda)$ are plotted in Figure 6. For the $\varepsilon(5f\pi)$, the average is over the spin−orbit split $5f\pi_{1/2}$ and $5f\pi_{3/2}$; for the nonbonding ϕ and δ orbitals, the average is over the 4 spin−orbit split 5f orbitals. The plot is between values of d(U-PC) = 3.00 bohr, or 1.6 Å and 1/d = 0.63 $Å^{-1}$, and d(U-PC) = 3.5 bohr, or 1.85 Å and 1/d = 0.54 $Å^{-1}$. The curves are nearly perfectly linear with rather similar slopes between 1.4 to 1.8 in units of Hartree-Angstroms. Although the potential of a PC (or a charged O anion) is proportional to 1/d, over the relatively small range of d in Figure 6, the

potential is closely represented with a linear plot. A similar linear behavior might be expected when we consider, below, plots of the $\varepsilon(5f\lambda)$ for UO_2^{2+}. The relatively small differences for the values and slopes of the $\varepsilon(5f\lambda)$ for $U(PC)_2$ are because the U orbitals are not concentrated at the U nucleus but have a nonspherical spatial extent.

The equivalent plot of the $\varepsilon(5f\lambda)$ for UO_2^{2+} is given in Figure 7 and there are considerable differences for all of the

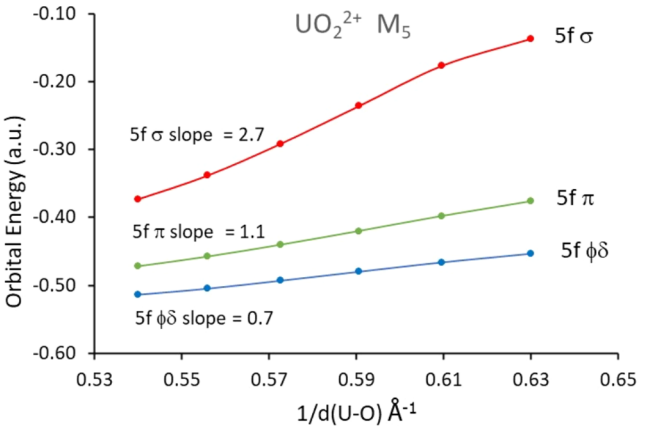

Figure 7. Plots of the 5fλ orbital energies, $\varepsilon(5f\lambda)$ in hartrees, for UO_2^{2+} for 1/d(U−O) in $Å^{-1}$ corresponding to d(U−O) between 1.6 to1.85 Å. see caption to Figure 6 and text.

5fλ. The 5f$\phi\delta$ curve is quite linear, as was the case for $U(PC)_2$, since these orbitals are nonbonding and cannot have any covalent O character. Note that the slope is half as large as that for the equivalent $\varepsilon(5f)$ curve for $U(VI)PC_2$ in Figure 6. One contribution to a smaller slope is a reduced charge from that of the $Q = -1.5$ used for the PCs. However, to account for large reduction in the slope would require that the effective anion charge in UO_2^{2+} would have to be about half of the PC = −1.5 used for the point charge model, which is very unlikely. Another reason is that there is also significant 6d occupation in the closed shell UO_2^{2+} g orbitals which makes the U(VI) less positive than U^{6+} and which lowers $\varepsilon(5f\lambda)$ more for shorter distances, larger values of 1/d(U−O), than for longer distances, smaller values of 1/d(U−O). This change in the 6d covalency offsets the changes in $\varepsilon(5f\lambda)$ due to the electric fields with changing distances. The d covalent character will be addressed in detail later. The $\varepsilon(5f\pi)$ curve has a larger slope and is somewhat less linear than the $\varepsilon(5f\phi\delta)$ curve. It is important that the slope for the $\varepsilon(5f\pi)$ curve is 50% larger that the slope of $\varepsilon(5f\phi\delta)$ compared to the only 15% increase for the $\varepsilon(5f\pi)$ slope for the $U(PC)_2$ curve. This is a strong indication that the covalent character of the 5fπ orbitals of UO_2^{2+} changes modestly as the d(U−O) changes. The changes in the linearity and slope of the $\varepsilon(5f\sigma)$ curve for UO_2^{2+} are much larger than for $\varepsilon(5f\pi)$. The slope for $\varepsilon(5f\sigma)$ is over 2.5 times larger than for $\varepsilon(5f\pi)$; this is strong and compelling evidence for a very large covalent character of the 5fσ orbital. This is not surprising since the directional properties of the 5fσ, along the internuclear axis, favor overlap and mixing with the O anion σ orbitals. However, the slope of the $\varepsilon(5f\sigma)$ shows that the open shell 5fσ has quite large covalent character. The projections, N_P, of the pure U^{6+} 5f orbitals on the open shell orbitals UO_2^{2+} of the excited $M_5 \rightarrow 5f$ configuration are shown in Figure 8; see Section II for details of these projections. They give a similar, confirming, view of the covalent character of the open shell orbitals as that obtained from the orbital energies discussed above. The projections are shown for each of the 7 5f spin orbitals although all the orbitals cannot be distinguished since the N_P for certain spinors are extremely similar. The $N_P(5f\phi_{5/2})$ and $N_P(5f\phi_{7/2})$ are essentially 1.0 showing that these orbitals are pure atomic orbitals. Indeed, they cannot be distinguished. The $N_P(5f\delta_{3/2})$ and $N_P(5f\delta_{5/2})$ are slightly smaller than 1.0 indicating that they have changed from the pure atomic orbitals for U^{6+} rather than having covalent character. However, the departure from $N_P = 1$ is quite small. There is modest covalency for the antibonding 5fπ and the $N_P(5f\pi_{1/2})$ can be distinguished from the $N_P(5f\pi_{3/2})$. The $N_P(5f\sigma_{1/2})$ shows substantial covalency and is in fact has more O character than 5f character; see ref 1. The small values for $N_P(5f\sigma_{1/2})$ are a clear indication that there is significant 5fσ

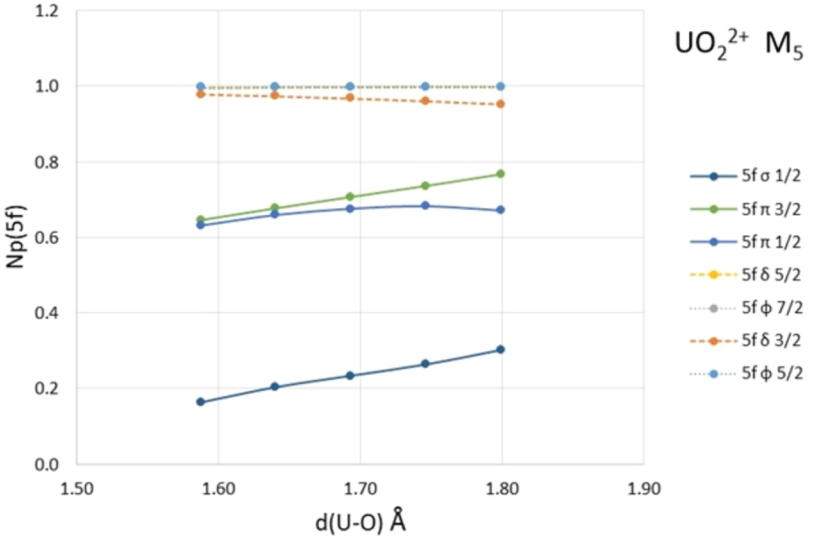

Figure 8. Projection of the U(5fλ) orbitals, denoted $N_p(5f)$, on the open shell orbitals of the M_5 configuration of UO_2^{2+} for d(U−O), in Å, between 1.6 and 1.8 Å. see text. Because the projections of the pair of orbitals 5f$\phi_{5/2}$ and 5f$\phi_{7/2}$ and the pair 5f$\delta_{5/2}$ and 5f$\delta_{5/2}$ are so nearly identical, these pairs cannot be resolved in the figure.

bonding character in the bonding closed shell orbitals that have σ symmetry.

An important concern, especially for the chemical bonding, is to understand the participation of the closed shell orbitals in the covalent bonding with the U(5f) and the U(6d) orbitals. Neither of these orbitals is occupied in the U(VI) cation. When we examine the closed shells, we are also able to contrast the covalent character in the initial, GS, state and in the multiplets of the excited states. One role that the covalent mixing in the excited states serves is to effectively screen the core hole[27−29] and this will be shown from the properties of the closed shell orbitals; further details of measures of the closed shell covalency are discussed in Section II.

The projection of the U(6d) and the U(5f) on the closed shells is shown in Figure 9 where the occupations are the

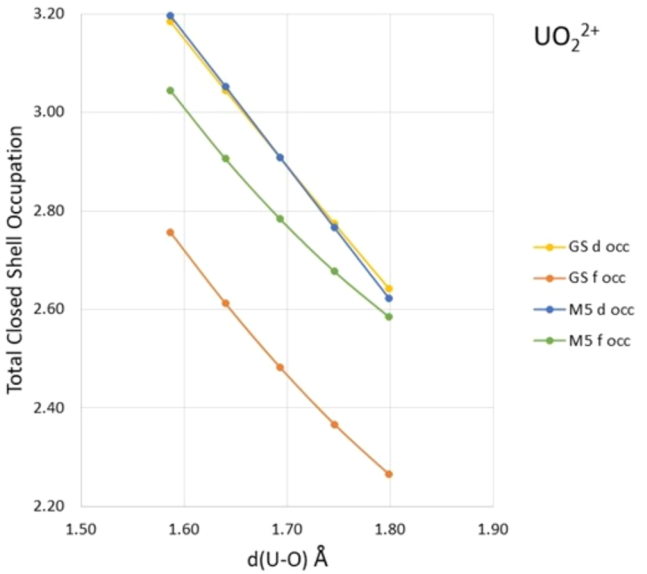

Figure 9. Projection of the U(5f) and U(6d) orbitals on the closed shell orbitals of the GS and M_5 configurations of UO_2^{2+} for d(U−O), in Å, between 1.6 and 1.8 Å. see text.

projections summed over all closed shell orbitals and includes the two electron occupations of these orbitals. They are also summed over the spin−orbit splittings of the 5f and 6d cation orbitals. The 6d and 5f are separated by symmetry where the 6d may be occupied only in g orbitals and the 5f only in u orbitals. As expected, there is a monotonic decrease in the closed shell occupations as the d(U−O) becomes larger; the decrease is ∼15% between the shortest and longest d(U−O) plotted. For the GS configuration orbitals, the U(6d) occupation is, at all d(U−O), somewhat larger than the U(5f) occupation. However, the changes from the occupations for the GS orbitals to those for the $M_5 \rightarrow$ 5f are quite important. While the U(6d) occupation is almost the same for both sets of closed shell orbitals, the U(5f) closed shell occupation for the $M_5 \rightarrow$ 5f excited configuration increases over the GS. This is an indication that the u symmetry U(5f) orbitals are more effective to screen the core hole by getting additional charge near the excited U than are the U(6d) orbitals. However, it is useful to show the role of the u closed shell orbitals by another, independent, test to ensure that the interpretation taken from the projections is correct and that there are no artifacts in the conclusion drawn from the projections.

This independent measure of the screening of the core excitation is obtained by examining the spatial extent of the closed shell charge density for both the GS and the $M_5 \rightarrow$ 5f configuration orbitals. We use as a measure of the spatial extent of an orbital, φ_i, the value of $\langle z \rangle_i$ where this expectation value of φ_i is made with the origin of z at the U center. With this choice of origin, the $\langle z^2 \rangle$ for an orbital dominantly on U is considerably smaller than the $\langle z^2 \rangle$ for an orbital dominantly on O; indeed, this is how the value of $\langle z^2 \rangle$ reflects the covalent character of an orbital. In Figure 10, the sum of $\langle z^2 \rangle_i$ made

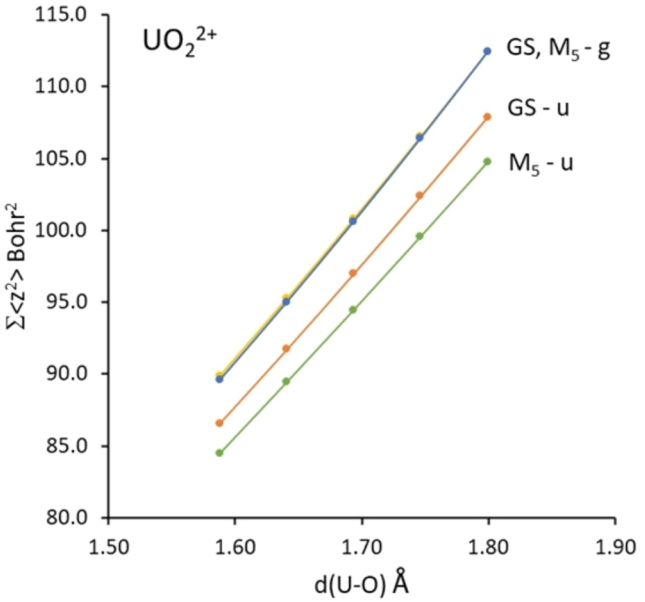

Figure 10. Sizes of the closed shell charge density, $\Sigma\langle z^2 \rangle$ in bohr^2, for the GS and $M_5 \rightarrow$ 5f configurations of UO_2^{2+} separated into g and u symmetry contributions for d(U−O), in Å, between 1.6 and 1.8 Å. see text.

separately over the closed shell orbitals of either g and u symmetry is given for several d(U−O) from 1.6 to 1.8 Å and for both the GS and the $M_5 \rightarrow$ 5f configurations. The spatial extent of the g orbitals provides information about covalent mixing with U(6d) and the extent of the u orbitals provides information about covalent mixing with U(5f). A detailed discussion of the use of $\langle z^2 \rangle$ is given in Section II. Clearly, if the covalent mixing of U(5f) or U(6d) in closed shell orbitals with large O character centered about the O anions increases and the O anion contribution decreases, the $\langle z^2 \rangle$ for that orbital will decrease. Conversely, if the covalent frontier U contributions decreased, the $\langle z^2 \rangle$ for that orbital, which has less U character and more O character will increase. All the different $\Sigma\langle z^2 \rangle$, increase significantly as d(U−O) increases. This is to be expected since a significant fraction of the 10 electrons formally associated with the O^{2-} anion will move with the anion, and as the anion moves away from the origin for $\langle z^2 \rangle$, which is at the U nucleus, the sum of $\Sigma\langle z^2 \rangle$ will be increased. However, besides the distance between the U cation and the O anions, other factors affect the sum. As discussed above, this will include changes in the covalent character of the orbitals as d(U−O) changes. The sums of the $\langle z^2 \rangle$ will also be affected by the degree of polarization of the orbitals induced by electric fields of the charges of the anions and cation and this polarization will also change with distance. However, the changes between the size of the charge density of the closed

shell orbitals for the GS and $M_5 \rightarrow 5f$ configurations provide direct information about the differences in the electronic structure of the GS and excited configurations. The sizes of the GS and $M_5 \rightarrow 5f$ configuration g charge distributions are very similar; indeed, so similar that it is difficult to distinguish the curves for the $\Sigma\langle z^2\rangle$ of the GS and $M_5 \rightarrow 5f$ configurations. On the other hand, the equivalent curves for the u closed shell orbitals can be easily distinguished in Figure 10. In this case, the u orbital curve for the $M_5 \rightarrow 5f$ configuration is lower than that for the GS by about 2 $bohr^2$ units. This indicates that charge in the u closed shell orbitals moves from the O anions toward the U cation when the $M_5 \rightarrow 5f$ excitation is made. A very rough estimate of the magnitude of charge that would have to change for a change in $\Sigma\langle z^2\rangle$ of 2 units is that an electron would have to move 2 bohr or 1 Å from O toward U to make this change. While this is not a dramatic change, it does indicate that the U(5f) orbitals participate in the screening of the 3d excitation while the U(6d) orbitals do not.

IV. SUMMARY

While the commonly used description of the XAS in actinyls is in terms of a one-electron excitation from the 3d shell into the unoccupied and antibonding 5f shell orbitals, see for example ref 21, our wave function analysis clearly shows that this assignment is simplified. In order to properly and accurately describe the XAS and the electronic structure of the excited states, it is essential to take the multiconfiguration, multi-determinantal character of the excited states into account. This essential multiconfiguration character raises the importance of coupling theoretical studies of the wave function character with measurements of the XAS in order to have a correct interpretation of their physical and chemical significance.

The multiconfiguration character can clearly be seen when the two active spaces that we have used: OSA, where the occupation of the closed shell orbitals are frozen, and OCSA, where excitations from these orbitals into the 5f space are allowed are compared. Despite the fact that the excited state electronic structure has an essential multiconfiguration character, it is possible to use an orbital analysis to describe the character of the wave functions. An important qualification is that one must make a judicious choice of the orbitals to be involved in the active spaces from which the configurations for the excited state wave functions are formed. Our analysis has shown that the properties of the orbitals and of the excited state wave functions have a strong dependence on the U−O distance. An important consequence of this dependence on distance is that the XAS theoretically predicted for different U−O distances in the linear UO_2^{2+} molecule have significantly different energy and intensity distributions. Based on this dependence, it is reasonable to propose that comparison of theoretical predictions of the XAS at the accurate OCSA level for different bond distances with experimental measurements of the XAS might be used to estimate the bond distances in uranyl and in other actinyls.

The theoretical studies in the present work have used several methods of analysis of the electronic structure that go well beyond the commonly used Mulliken population analysis.[30,31] In particular, the projection of the U(5f) and U(6d) fragment orbitals of the isolated U cation on the orbitals of UO_2^{2+} has been used to identify the covalent character of the UO_2^{+2} orbitals. Furthermore, the U orbital occupations of the many-body OSA and OCSA wave functions of the excited states have been used to provide a chemical understanding of these many-body effects. In addition, the sizes of orbital and total charge distributions and the orbital energies have also provided useful measures of how the uranyl electronic structure changes with bond distance. These methods of analysis significantly extend the power of computational electronic structure studies from simply trying to replicate observed values to understanding the origins of these properties in the electronic structure and interactions.

ASSOCIATED CONTENT

Data Availability Statement

The data that supports the findings of this study are available within the article.

AUTHOR INFORMATION

Corresponding Authors

Paul S. Bagus − *Department of Chemistry, University of North Texas, Denton, Texas 76203-5017, United States;* orcid.org/0000-0002-5791-1820; Email: Paul.Bagus@unt.edu

Robert Polly − *Karlsruhe Institute of Technology (KIT), Institute for Nuclear Waste Disposal (INE), D-76021 Karlsruhe, Germany*; Email: robert.polly@kit.edu

Authors

Connie J. Nelin − *Consultant, Austin, Texas 78730, United States*

Bianca Schacherl − *Karlsruhe Institute of Technology (KIT), Institute for Nuclear Waste Disposal (INE), D-76021 Karlsruhe, Germany;* orcid.org/0000-0003-4542-0108

Tonya Vitova − *Karlsruhe Institute of Technology (KIT), Institute for Nuclear Waste Disposal (INE), D-76021 Karlsruhe, Germany;* orcid.org/0000-0002-3117-7701

Notes

The authors declare no competing financial interest.

ACKNOWLEDGMENTS

P.S.B. gratefully acknowledges support from the U.S. Department of Energy, Office of Science, Office of Basic Energy Sciences, Chemical Sciences, Geosciences, and Biosciences (CSGB) Division through its Geosciences program at Pacific Northwest National Laboratory (PNNL). PNNL is a multi-program national laboratory operated for the DOE by Battelle Memorial Institute under contract no. DE-AC05-76RL01830. T.V., B.S., and P.S.B. acknowledge funding from the European Research Council (ERC) Consolidator Grant 2020 under the European Union's Horizon 2020 research and innovation program. (Grant agreement no. 101003292)

REFERENCES

(1) Bagus, P. S.; Nelin, C. J.; Rosso, K. M.; Schacherl, B.; Vitova, T. Electronic Structure of Actinyls: Orbital Properties. *Inorg. Chem.* **2024**, *63*, 1793.

(2) Bagus, P. S.; Nelin, C.; Schacherl, B.; Vitova, T. Actinyl Electronic Structure Probed by Xas: The Role of Many Body Effects. *Inorg. Chem.* **2024**, *63*, 13202.

(3) Rothe, J.; Altmaier, M.; Dagan, R.; Dardenne, K.; Fellhauer, D.; Gaona, X.; González-Robles Corrales, E.; Herm, M.; Kvashnina, K. O.; Metz, V.; et al. Fifteen Years of Radionuclide Research at the Kit

Synchrotron Source in the Context of the Nuclear Waste Disposal Safety Case. *Geosciences* **2019**, *9*, 91.
(4) Neidig, M. L.; Clark, D. L.; Martin, R. L. Covalency in F-Element Complexes. *Coord. Chem. Rev.* **2013**, *257*, 394−406.
(5) Kaltsoyannis, N. Does Covalency Increase or Decrease across the Actinide Series? Implications for Minor Actinide Partitioning. *Inorg. Chem.* **2013**, *52*, 3407−3413.
(6) Polly, R.; Schacherl, B.; Rothe, J.; Vitova, T. Relativistic Multiconfigurational Ab Initio Calculation of Uranyl 3d4f Resonant Inelastic X-Ray Scattering. *Inorg. Chem.* **2021**, *60*, 18764−18776.
(7) Vitova, T.; Faizova, R.; Amaro-Estrada, J. I.; Maron, L.; Pruessmann, T.; Neill, T.; Beck, A.; Schacherl, B.; Tirani, F. F.; Mazzanti, M. The Mechanism of Fe Induced Bond Stability of Uranyl(V). *Chem. Sci.* **2022**, *13*, 11038−11047.
(8) Sergentu, D.-C.; Duignan, T. J.; Autschbach, J. Ab Initio Study of Covalency in the Ground Versus Core-Excited States and X-Ray Absorption Spectra of Actinide Complexes. *J, Phys. Chem. Lett.* **2018**, *9*, 5583−5591.
(9) Sergentu, D.-C.; Autschbach, J. Covalency in Actinide(Iv) Hexachlorides in Relation to the Chlorine K-Edge X-Ray Absorption Structure. *Chem. Sci.* **2022**, *13*, 3194−3207.
(10) Misael, W. A.; Severo Pereira Gomes, A. Core Excitations of Uranyl in Cs2uo2cl4 from Relativistic Embedded Damped Response Time-Dependent Density Functional Theory Calculations. *Inorg. Chem.* **2023**, *62*, 11589−11601.
(11) Ramanantoanina, H.; Kuri, G.; Martin, M.; Bertsch, J. Study of Electronic Structure in the L-Edge Spectroscopy of Actinide Materials: Uo2 as an Example. *Phys. Chem. Chem. Phys.* **2019**, *21*, 7789−7801.
(12) Sergentu, D.-C.; Autschbach, J. X-Ray Absorption Spectra of F-Element Complexes: Insight from Relativistic Multiconfigurational Wavefunction Theory. *Dalton Trans.* **2022**, *51*, 1754−1764.
(13) Konecny, L.; Vicha, J.; Komorovsky, S.; Ruud, K.; Repisky, M. Accurate X-Ray Absorption Spectra near L- and M-Edges from Relativistic Four-Component Damped Response Time-Dependent Density Functional Theory. *Inorg. Chem.* **2022**, *61*, 830−846.
(14) Stanistreet-Welsh, K.; Kerridge, A. Bounding [Ano2]2+ (an = U, Np) Covalency by Simulated O K-Edge and an M-Edge X-Ray Absorption near-Edge Spectroscopy. *Phys. Chem. Chem. Phys.* **2023**, *25*, 23753.
(15) Amidani, L.; Retegan, M.; Volkova, A.; Popa, K.; Martin, P. M.; Kvashnina, K. O. Probing the Local Coordination of Hexavalent Uranium and the Splitting of 5f Orbitals Induced by Chemical Bonding. *Inorg. Chem.* **2021**, *60*, 16286−16293.
(16) Allen, P. G.; Bucher, J. J.; Shuh, D. K.; Edelstein, N. M.; Reich, T. Investigation of Aquo and Chloro Complexes of Uo22+, Npo2+, Np4+, and Pu3+ by X-Ray Absorption Fine Structure Spectroscopy. *Inorg. Chem.* **1997**, *36*, 4676−4683.
(17) Wahlgren, U.; Moll, H.; Grenthe, I.; Schimmelpfennig, B.; Maron, L.; Vallet, V.; Gropen, O. Structure of Uranium(Vi) in Strong Alkaline Solutions. A Combined Theoretical and Experimental Investigation. *J. Phys. Chem. A* **1999**, *103*, 8257−8264.
(18) Burns, G. *Introduction to Group Theory with Applications*; Academic Press: New York, 1977.
(19) Saue, T. Relativistic Hamiltonians for Chemistry: A Primer. *ChemPhysChem* **2011**, *12*, 3077−3094.
(20) Visscher, L.; Visser, O.; Aerts, P. J. C.; Merenga, H.; Nieuwpoort, W. C. Relativistic Quantum Chemistry: The Molfdir Program Package. *Comput. Phys. Commun.* **1994**, *81*, 120−144.
(21) Vitova, T.; Pidchenko, I.; Fellhauer, D.; Bagus, P. S.; Joly, Y.; Pruessmann, T.; Bahl, S.; Gonzalez-Robles, E.; Rothe, J.; Altmaier, M.; et al. The Role of the 5f Valence Orbitals of Early Actinides in Chemical Bonding. *Nat. Commun.* **2017**, *8*, No. 16053.
(22) Bethe, H. A.; Salpeter, E. W. *Quantum Mechanics of One- and Two-Electron Atoms*; Academic Press, 1957.
(23) Thompson, A.; Atwood, D.; Gullikson, E.; Howells, M.; Kim, K.-J.; Kirz, J.; Kortright, J.; Lindau, I.; Liu, Y.; Pianetta, P., et al.., *X-Ray Data Booklet, Lbnl/Pub-490*, Lawrence Berkeley National Lab, 2009; for Access to This Publication See Also Url: Http://Xdb.Lbl.Gov.
(24) Löwdin, P. O. Quantum Theory of Many-Particle Systems. I. Physical Interpretations by Means of Density Matrices, Natural Spin-Orbitals, and Convergence Problems in the Method of Configurational Interaction. *Phys. Rev.* **1955**, *97*, 1474−1489.
(25) Sherwood, P. M. A. Rapid Evaluation of the Voigt Function and Its Use for Interpreting X-Ray Photoelectron Spectroscopic Data. *Surf. Interface Anal.* **2019**, *51*, 254−274.
(26) Campbell, J. L.; Papp, T. Widths of the Atomic K - N7 Levels. *At. Data Nucl. Data Tables* **2001**, *77*, 1−56.
(27) Bagus, P. S.; Ilton, E. S.; Nelin, C. J. The Interpretation of Xps Spectra: Insights into Materials Properties. *Surf. Sci. Rep.* **2013**, *68*, 273−304.
(28) Bagus, P. S.; Ilton, E. S.; Nelin, C. J. Extracting Chemical Information from Xps Spectra: A Perspective. *Catal. Lett.* **2018**, *148*, 1785−1802.
(29) Bagus, P. S.; Nelin, C. J.; Brundle, C. R. Chemical Significance of X-Ray Photoelectron Spectroscopy Binding Energy Shifts: A Perspective. *J. Vac. Sci. Technol., A* **2023**, *41*, No. 068501.
(30) Mulliken, R. S. Electronic Population Analysis on LCAO−MO Molecular Wave Functions. I. *J. Chem. Phys.* **1955**, *23*, 1833−1840.
(31) Mulliken, R. S. Electronic Population Analysis on LCAO−MO Molecular Wave Functions. II. Overlap Populations, Bond Orders, and Covalent Bond Energies. *J. Chem. Phys.* **1955**, *23*, 1841−1846.